

See discussions, stats, and author profiles for this publication at: <https://www.researchgate.net/publication/322888743>

"Etchability Dependence of InOx and ITO Thin Films by Plasma Enhanced Reactive Thermal Evaporation on Structural Properties and....

Conference Paper · November 2017

CITATIONS

0

READS

4

1 author:



Carlos NUNES Carvalho

New University of Lisbon

180 PUBLICATIONS 619 CITATIONS

SEE PROFILE



Etchability Dependence of InOx and ITO Thin Films by Plasma Enhanced Reactive Thermal Evaporation on Structural Properties and Deposition Conditions

Journal:	<i>MRS Advances</i>
Manuscript ID	MRSF17-2790574.R1
Manuscript Type:	Symposium NM5
Date Submitted by the Author:	n/a
Complete List of Authors:	Amaral, Ana; Universidade de Lisboa Instituto Superior Tecnico; Universidade de Lisboa Centro de Fisica e Engenharia de Materiais Avancados Lavareda, G.; Universidade Nova de Lisboa Centro de Tecnologias e Sistemas; Universidade Nova de Lisboa, Departamento de Ciências de Materiais Carvalho, C.; Universidade de Lisboa Centro de Fisica e Engenharia de Materiais Avancados; Universidade Nova de Lisboa, Departamento de Ciências de Materiais André, Vânia; Universidade de Lisboa Instituto Superior Tecnico Vygranenko, Yuri; Universidade Nova de Lisboa Centro de Tecnologias e Sistemas Fernandes, Miguel; ISEL; Universidade Nova de Lisboa Centro de Tecnologias e Sistemas Brogueira, Pedro; Universidade de Lisboa Centro de Fisica e Engenharia de Materiais Avancados; Instituto Politecnico de Lisboa, Departamento de Engenharia Electrotécnica e de Computadores
Keywords:	transparent conductor, thin film, plasma deposition

Etchability Dependence of InO_x and ITO Thin Films by Plasma Enhanced Reactive Thermal Evaporation on Structural Properties and Deposition Conditions

Ana Amaral^{1,2*}, G. Lavareda^{3,4}, C. Nunes de Carvalho^{2,3}, V. André⁵, Yuri Vygranenko⁴, M. Fernandes^{4,6}, Pedro Brogueira^{1,2}

¹ Departamento de Física, Instituto Superior Técnico, Universidade de Lisboa, Portugal.

² Centro de Física e Engenharia de Materiais Avançados (CeFEMA), Instituto Superior Técnico, Universidade de Lisboa, Portugal.

³ Departamento de Ciências de Materiais, Faculdade de Ciências e Tecnologia, Universidade Nova de Lisboa, Portugal.

⁴ Centro de Tecnologia e Sistemas, Faculdade de Ciências e Tecnologia (CTS), Universidade Nova de Lisboa, Portugal.

⁵ Centro de Química Estrutural (CQE), Instituto Superior Técnico, Universidade de Lisboa, Portugal.

⁶ Departamento de Engenharia Electrotécnica e de Computadores, Instituto Superior de Engenharia de Lisboa, Instituto Politécnico de Lisboa, Portugal.

* Phone: +351 218419279; e-mail: ana.de.amaral@tecnico.ulisboa.pt

ABSTRACT

Indium oxide (InO_x) and indium tin oxide (ITO) thin films were deposited on glass substrates by plasma enhanced reactive thermal evaporation (PERTE) at different substrate temperatures. The films were then submitted to two etching solutions with different chemical reactivity: i) HNO₃ (6%), at room temperature; ii) HCl (35%): (40 °Bé) FeCl₃ (1:1), at 40 °C. The dependence of the etchability of the films on the structural and deposition conditions is discussed. Previously to etching, structural characterization was made. X-ray diffraction showed the appearance of a peak around 2θ=31° as the deposition temperature increases from room temperature to 190 °C, both for ITO and InO_x. AFM surface topography and SEM micrographs of the deposited films are consistent with the structural properties suggested by X-ray spectra: as the deposition temperature increases, the surface changes from a finely grained structure to a material with a larger-sized grain or/and agglomerate structure of the

order of 250-300 nm. The roughness R_q varies from 0.74 nm for the amorphous tissue to a maximum of 10.83 nm for the sample with the biggest crystalline grains. Raman spectra are also presented.

INTRODUCTION

Transparent conductive oxides (TCOs) thin films (first appearance in 1907 by Bädeker [1]), frequently used in various optoelectronic device fabrication, are materials whose physical, structural and chemical properties are still subject of investigation in present times [2-3]. Indium oxide (InO_x) and indium tin oxide (ITO) thin films are TCO materials both with their own properties, strongly dependent upon their oxidation state (stoichiometry), quantity of impurities trapped in the film and film deposition processes and conditions [4]. For this work, conductive oxide thin films were deposited by radio-frequency plasma enhanced reactive thermal evaporation (rf-PERTE) on glass substrates [5]. The variation of their characteristics, e.g., (1) surface morphology and (2) structure (grain or agglomerate presence) with substrate temperature (from 25 up to 190 °C) is studied. The etch rate as a function of substrate temperature has been also determined for two types of chemical etching solutions.

EXPERIMENTAL

Samples ($2.5 \times 2.5 \text{ cm}^2$) of indium oxide (InO_x) and indium tin oxide (ITO) were deposited on glass substrates previously cleaned with ion free detergent and rinsed with ultra-pure water ($\rho = 18.2 \text{ M}\Omega\cdot\text{cm}$). The deposition process used for both materials was radio-frequency plasma (13.56 MHz) enhanced reactive thermal evaporation technique (rf-PERTE) using indium tear drops and an indium-tin alloy (80%:20%), respectively, as the material source in the crucible. All the other deposition conditions were kept nearly constant and referred elsewhere [5]. Samples were deposited at the following temperatures: 25 ± 1 , 110 ± 1 , 130 ± 1 , 150 ± 6 , 170 ± 2 and 190 ± 2 °C. Post deposition annealing treatments were not used whatsoever. The thickness of the films is within the range of 100-160 nm by a Dektak III profilometer. The sheet resistance was measured using Veeco FPP5000 four-point gauge. Scanning Electron Microscopy (SEM) and glancing incidence X-ray Diffraction (GIXRD) are the main characterization methods complemented with Raman and AFM techniques. A LabRAM HR Evolution Raman microscope from Horiba Scientific, with a 532 nm green laser and a 600 gr/mm grating was used to obtain the spectra in the 150 to 1800 cm^{-1} Raman shift range for samples deposited on AF45 substrates. A Dimension 3100 SPM with a Nanoscope IIIa controller from Digital Instruments (DI) was used for the AFM measurements. The measurements were performed in tapping mode (TM) under ambient conditions. A commercial tapping mode etched silicon probe from Bruker and a $90 \times 90 \text{ }\mu\text{m}^2$ scanner were used.

The etchability of both films is verified using two chemical etching solutions: (1) HNO_3 (6%) used at room temperature and (2) FeCl_3 (40 °Bé):HCl (37%), in a 50% proportion, used at 40 °C. Solution (1) has been optimized previously for low temperature deposited samples, giving typical etch rates of 5-10 Å/s. Solution (2) is a standard ITO etching solution [6-7]. Both processes were done by the usual dip method. By knowing the etched thickness and the time of etching, the etch rate can be easily calculated. SEM measurements are made using a Field Emission Scanning Electron Microscope (SEM) JEOL JSM-7001F. Grazing-incidence X-ray diffraction (GIXRD) measurements are performed using a D8 ADVANCE diffractometer with

DAVINCI.DESIGN and a LINXEYE-XE detector ($\text{Cu K}\alpha\lambda=1.54\text{\AA}$) in the grazing incidence geometry, with an incident beam angle of 1.5° .

RESULTS AND DISCUSSION

For both TCOs in the present study, the value of electrical resistivity is within the range $(3-11)\times 10^{-4}\ \Omega\text{cm}$. Figure 1(a) shows the variation of etch rate for InO_x and ITO thin films with substrate temperature, using the etching solution of $\text{HNO}_3(6\%)$, at room temperature. The etching rate values decrease slowly with increasing substrate temperature up to 130°C , and the exponential decrease over three orders of magnitude is observed in the range of 150 to 190°C . Besides, from room temperature up to $(130)^\circ\text{C}$ the etch rate values of InO_x films are slightly higher than those of ITO films, and from 150 to 190°C , the etch rate values of the ITO films are higher than those of InO_x . The significant change verified in their morphology and the presence of tin (Sn) as the doping impurity (it is known that tin segregates to grain boundaries in response to temperature increase [8]) maybe responsible for that difference. The fine grained structure observed at low substrate temperatures gives rise to larger-sized grain structure material at high substrate temperatures, more evident for ITO films [9].

Figure 1(b) shows the variation of etch rate of InO_x and ITO thin films with substrate temperature for the etching solution $\text{FeCl}_3(40^\circ\text{Bé})\text{:HCl}(35\%)(1\text{:}1)$, performed at 40°C . In this case, the etching rate values obtained are much higher than the ones obtained in the previous study.

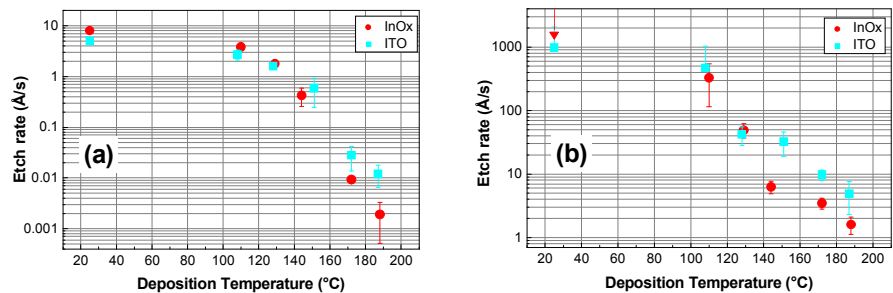


Figure 1. Etch rate variation of InO_x and ITO thin films with substrate temperature for two etching solutions: (a) $\text{HNO}_3(6\%)$ in water at room temperature, and (b) $\text{FeCl}_3(40^\circ\text{Bé})\text{:HCl}(35\%)(1\text{:}1)$ at 40°C

The higher chemical reactivity of the etching solution combined with the higher temperature of the etching process (40°C) are the main factors for this increase. Nevertheless, the etch rate curves are of almost the same shape over the studied temperature range. Middle range substrate temperatures ($110-130^\circ\text{C}$), give rise to almost identical etch rate values for both films. Above 150°C , the etch rate values of the ITO films become higher than those of the InO_x films. These comments become clearer, observing Figures 2 to 4, with the results of SEM and GIXRD. The etch rate of the InO_x sample deposited at room temperature could not be measured since the etching time was less than one second. A different marker (triangle) is used to note the minimum of the error bar, corresponding to 1 s.

Figure 2 shows grazing-incidence X-ray diffraction patterns of InO_x and ITO [10] thin films for the two extreme substrate temperatures in the range 25-190 °C. Curves 1 and 3 indicates that low temperature samples are mostly amorphous, while the layers deposited at 190 °C are highly crystalline with preferable nanocrystal orientation of (222). Raman spectra also indicate the increase in film crystallinity that is associated with the height of the spectral band centered at 560 cm^{-1} .

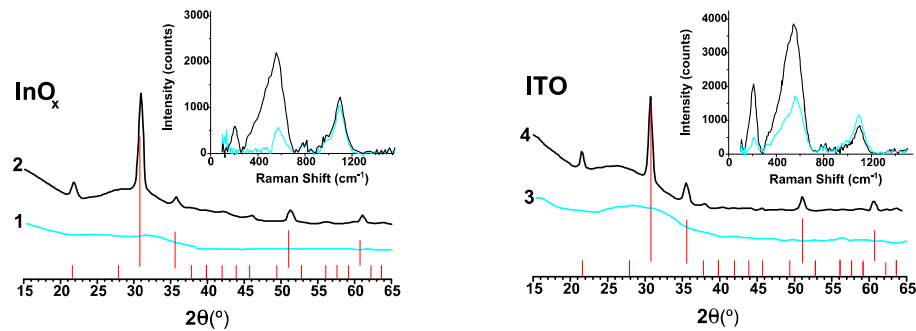


Figure 2. Grazing-incidence X-ray diffraction measurements for InO_x and ITO deposited at ambient temperature (curves 1 and 3) and 190 °C (curves 2 and 4), compared with the patterns of materials from the Crystallography Open Database (COD1010341). The insets show Raman spectra of the films after subtracting the baseline.

Figure 3 shows SEM micrographs of InO_x (A, C, E, G) and ITO (B, D, F, H) films as a function of the substrate temperature. As can be seen, high-temperature materials present big crystal islands inserted in grain-shaped domains characterized by small crystallites, grown in the same direction (Figures 3 E to H). These domains are particularly evident in Figure 3 F and G. The shape of the big crystal islands is quite different for InO_x and ITO films. Probably the presence of tin in the ITO films may be responsible for this, during the coalescence of small crystallites.

Low and medium temperature material, deposited from room temperature up to $\approx 150\text{ °C}$, show close-packed small crystallites, although the structure compactness seems to be higher at 150 °C , namely in InO_x films (Figure 3 A and C). Figure 4 shows an example of InO_x film deposited at 172 °C after being submitted to a partial etching process. As can be seen here, the high-temperature materials are firstly etched preferentially in the grain boundaries, followed by the etching of the tissue under those grains, causing the peeling phenomenon. This indicates a bulk coalescence of the small crystallites having the same orientation, forming a monocrystal (grain).

The roughness values (R_q) deduced from AFM are summarized in Table I. It varies from 0.74 nm for the amorphous tissue deposited at room temperature to a maximum for 10.83 nm for the sample with the biggest crystalline grains, deposited at 190 °C .

Table I. Roughness (R_q) of InO_x and ITO deduced from AFM data

Temperature (°C)	25	150	170	190
InO_x roughness (nm)	0.74	0.90	1.31	5.25
ITO roughness (nm)	0.91	1.09	1.05	10.83

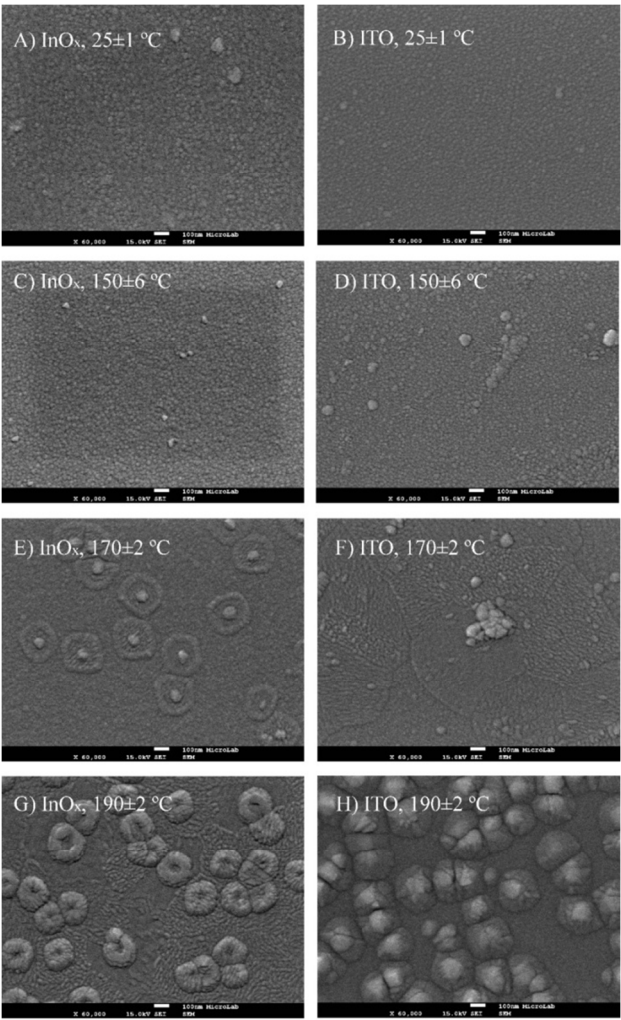


Figure 3. SEM micrographs of InO_x (A, C, E, G) and ITO (B, D, F, H) films deposited by PERTE on glass substrates as a function of substrate temperature

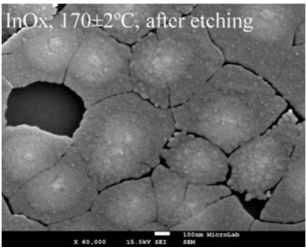


Figure 4. SEM micrograph of an InO_x sample after partial etching in solution #2. Macroscopic aspect shows hazy transparency.

CONCLUSIONS

The etch rate values for both types of films decrease with the increasing substrate temperature for both chemical solutions. High controllability of the etching rate for ITO and InO_x thin films deposited at various temperatures is demonstrated. The etching rate curves are of the same shape for both materials and chemical solutions (in the range of temperature 25 to 190 °C), although the etching rate values are much higher for the HCl/FeCl₃ etching process. For both materials there is a critical temperature, approximately at ≈150 °C, where a more abrupt change in the etch rate values is observed. Above this temperature, the ITO films exhibit higher etch rate than that for the InO_x films. These conclusions are in good agreement with SEM and GIXRD studies as both materials show a close-packed small crystallites structure below the critical temperature, while for higher substrate temperatures, the larger-sized grain or/and agglomerate structure is dominant.

ACKNOWLEDGMENTS

The authors gratefully acknowledge T. Duarte for the X-ray diffraction facilities, “Fundação para a Ciência e a Tecnologia” for funding through a pluriannual contract with CeFEMA (UID/CTM/04540/2013) and fellowship (SFRH/BPD/102217/2014) for financial support of this research.

REFERENCES

1. K. Bädeker, *Annals of Physics* (Leipzig) **22**, 749-766 (1907).
2. A. Alyamani and N. Mustapha, *Thin Solid Films* **611**, 27-32 (2016).
3. S. Elmas, S. Korkmaz, and S. Pat, *Applied Surface Science* **276**, 641-645 (2013).
4. A.L. Dawar and J.C. Joshi, *Journal of Materials Science* **19**, 1-23 (1984).
5. C. Nunes Carvalho, G. Lavareda, P. Parreira, J. Valente, A. Amaral, and A.M. Botelho do Rego, *J. Non-Crystalline Solids* **354**, 1643-1647 (2008).
6. *Transparent Conductive Film on Glass Plate (I.T.O. Plate)* (HOYA EUROPE B.V., London, 1990).
7. J.E.A.M. van den Meerakker, P.C. Baarslag, and M. Scholten, *J. Electrochem. Soc.* **142** (7), 2321-2325 (1995).
8. M.V. Hohmann, A. Wachau, and A. Klein, *Solid State Ionics* **262**, 636-639 (2014).
9. A.S. Ryzhikov, R.B. Vasiliev, M.N. Rumyantseva, L.I. Ryabova, G.A. Dosovitsky, A.M. Gilmudinov, V.F. Kozlovsky, and A.M. Gaskov, *Materials Science & Engineering* **B96**, 268-274 (2002).
10. S. Grazulis, D. Chateigner, R.T. Downs, A.T. Yokochi, M. Quiros, L. Lutterotti, E. Manakova, J. Butkus, P. Moeck, and A. Le Bail, *J. Appl. Cryst.* **42**, 726-729 (2009).